

## Three-Component Dust Models for Interstellar Extinction

C. Muthumariappan

*Vainu Bappu Observatory, Indian Institute of Astrophysics, Kavalur 635 701, India.  
e-mail: muthu@iiap.res.in*

Received 2009 March 23; accepted 2010 January 13

**Abstract.** Interstellar extinction curves obtained from the ‘extinction without standard’ method were used to constrain the dust characteristics in the mean ISM ( $R_V = 3.1$ ), along the lines of sight through a high latitude diffuse molecular cloud towards HD 210121 ( $R_V = 2.1$ ) and in a dense interstellar environment towards the cluster NGC 1977 ( $R_V = 6.42$ ). We have used three-component dust models comprising silicate, graphite and very small carbonaceous grains (polycyclic aromatic hydrocarbons) following the grain size distributions introduced by Li & Draine in 2001. It is shown that oxygen, carbon and silicon abundances derived from our models are closer with the available elemental abundances for the dust grains in the ISM if F & G type stars atmospheric abundances are taken for the ISM than the solar. The importance of very small grains in modelling the variation of interstellar extinction curves has been investigated. Grain size distributions and elemental abundances locked up in dust are studied and compared at different interstellar environments using these three extinction curves. We present the albedo and the scattering asymmetry parameter evaluated from optical to extreme-UV wavelengths for the proposed dust models.

*Key words.* Dust extinction—ISM: abundances—ISM.

### 1. Introduction

The nature of the interstellar dust is completely characterized by its composition, morphology, size distribution, and elemental abundances in dust. Dust characteristics govern several physical and chemical phenomena in the ISM and act as a tracer of local interstellar environmental conditions. Observational signatures to characterize the ISM dust are the wavelength dependence of the interstellar extinction, IR emission, albedo and polarisation. The UV extinction bump at 2175 Å was first detected by Stecher (1965) and its interstellar origin was confirmed by Bless & Seville (1972), which is a most important signature of the interstellar dust to constrain its chemistry. The wavelength dependence of interstellar extinction is due to scattering and strongly constrains the grain size distribution, whereas the spectral features of the extinguished light reveal the chemical composition of the grains as it is due to resonant absorption. Interstellar extinction varies with the direction significantly implying that the properties of interstellar dust are not uniform in the Galaxy. The FWHM of the 2175 Å absorption

feature has a variation of 12%, whereas, the central wavelength shows a variation of only 0.46%. The strength of this absorption feature too varies significantly across different lines of sight in the Galaxy implying a chemical inhomogeneity. The slope of the underlying optical and UV extinction shows a wide variation. These differences in the observed extinction curves provide a clear challenge in developing interstellar dust models.

Interstellar dust models have evolved as the observational data have advanced, and the most popular dust model was proposed by Mathis *et al.* (1977, MRN models hereafter). This model constitutes spherical graphite and silicate dust particles following a power law grain size distribution going as  $a^{-3.5}$  with  $0.005 \mu$  and  $0.25 \mu$  respectively being the minimum and maximum sizes of the particles. Models were also calculated with spheroidal, composite, porous grains (Vaidya *et al.* 2006) following MRN grain size distribution. Though the average interstellar extinction was well reproduced by these models, the observed variation in the extinction curve and in the  $2175 \text{ \AA}$  interstellar feature could not be explained satisfactorily by the large (larger than  $100 \text{ \AA}$ ) graphite grains. In addition, bare graphite demands large amounts of carbon to reproduce the  $2175 \text{ \AA}$  feature than that available for the ISM dust. If solar composition of elements is assumed for the ISM, the MRN model with spherical dust components needs all the interstellar carbon, magnesium, silicon and iron locked up in dust. Further evidence for the incompleteness of the dust models following MRN grain size distribution comes from the IRAS observation which shows an excess of  $12 \mu$  and  $25 \mu$  emission from the ISM than expected. This excess of emission was attributed to the dust particles extended to very small sizes, down to  $\sim 5 \text{ \AA}$  and heated to a temperature of  $\sim 100 \text{ K}$  by the average ISM radiation field (Draine & Anderson 1985). As the composite grain models of Vaidya *et al.* (2006) do not consider the very small grain population, the observed UIR emission bands in the ISM cannot be reproduced by this model. From the observed solid state UIR emission feature in the ISM, Allamandola *et al.* (1985) identified that these very small grains undergoing temperature fluctuation are indeed PAH molecules. Observation of dust correlated microwave emission was also attributed to the very small grain population in the ISM by Draine & Lazarian (1998).

It is now recognized that the interstellar grain population can include a substantial amount of very small grains with PAH composition and a significant fraction of the ISM carbon is locked into the PAH molecules. Variation in the Galactic extinction curves were largely seen in the UV and Far-UV regions which are provided by the very small grain population. Li & Draine (2001) suggested from their model calculations to explain the diffuse Galactic emission that carbon abundance of  $\sim 50 \text{ ppm}$  is required in PAH in the ISM. PAH, having strong absorption in the  $2000\text{--}2500 \text{ \AA}$  wavelength region, is also a potential carrier of the  $2175 \text{ \AA}$  interstellar absorption feature. The observed variations in the FWHM of the feature would result from differences in the PAH mix at different lines of sight. The compulsion to include very small grains with PAH population in the ISM needed a revision on the ISM dust models. Li & Greenberg (1997) included PAH with cylindrical silicates coated with organic refractory mantle for their calculation of the extinction curve meeting the solar abundance constrains. Zubko *et al.* (2004) have shown that dust models having silicate, graphite and PAH as components can fit the average interstellar extinction with a relatively low atomic abundance in dust than that which the MRN model demands. Their dust model, which includes composite grain containing silicates and organic refractory materials, requires

even lower atomic abundance than that expected in dust. In this paper, we analyse the extinction curves along different lines of sight in the ISM using three-component dust models comprising bare silicate, graphite and PAH to meet the constraints obtained from various observations.

## 2. Observed extinction

The wavelength dependent interstellar extinction curve was parameterized by Fitzpatrick & Massa (2005) and they revised their parameterization later (Fitzpatrick & Massa 2007, FM07 hereafter). They have used a new technique called ‘extinction without standards’ to obtain the observed extinction. Unlike previous parameterizations by several authors (Cardelli *et al.* 1989, CCM hereafter; Fitzpatrick 1999) who have used data obtained from ‘pair method’, this involves determining the shapes of UV through IR interstellar extinction by modelling the observed spectral energy distribution of reddened early-type stars. This method has an advantage over results generated using the standard ‘pair method’ by virtually eliminating the spectral mismatch of stars as a source of error in determining extinction and provides an increased accuracy and precision on extinction curve with a more reliable estimate on the uncertainty. FM07 have parameterized 328 Galactic interstellar extinctions affecting normal, near main sequence B and late O type stars using data from IUE low resolution spectrophotometry, and ground based Optical ( $U$ ,  $B$ ,  $V$  bands from General Catalogue of Photometric Data) and near-IR ( $J$ ,  $H$ ,  $K$  bands from  $2\mu$  All Sky Survey) photometry. The observed extinction curves for our study were produced using the published parameters of those lines of sight by FM07. We have taken three lines of sight namely the average ISM extinction ( $R_V = 3.1$ ), the line of sight passing through a high latitude diffuse molecular cloud towards HD 210121 which has the lowest value of  $R_V (= 2.1)$ , and the line of sight passing through a dense interstellar environment with a very large value of  $R_V (= 6.42)$  towards HD 37022 in the cluster NGC 1977.

## 3. Methodology

From their quantitative model calculation, Li & Draine (2001) have shown that the diffuse Galactic emission can be best reproduced by considering a sum of two log normal size distribution for the very small dust grains in addition to an adjustable power law size distribution for the classical grains. Later, Weingartner & Draine (2001, WD01 hereafter) have used the same functional form of size distribution to examine the interstellar extinction curves. The observed extinction  $A(\lambda, R_V)$  for their study was adapted from the  $R_V$  dependent extinction curve derived by Fitzpatrick (1999), which is based on the analysis of the extinction curves derived from the ‘pair method’ (Fitzpatrick & Massa 1986, 1988). From their study, FM07 have concluded that there is no global one parameter family of extinction curves, although extremely large values of  $R_V$  curves display distinctive properties. This indicates that the environmental processes that modify grain sizes are size selective in the ISM. Hence, the study of WD01 needs to be reconsidered with more appropriate observed extinction curve in addition to an adequate functional form of grain size distribution for the interstellar dust, which we intend to make.

Our present study is similar to the work of WD01, apart from the data on which the models were applied, where we consider bare spherical grains and focus on the

grain size distribution and the inclusion of very small grains. For a comparative study of dust properties, viz., grain size distributions, albedo, scattering asymmetry parameter and dust based abundances at different interstellar environments this method is adequate. However, extension of this work with vacuum included spheroidal grains is in progress to derive more accurate parameter values, which also should yield the same conclusions reached by this work, even if the derived values will be different, as it proportionally impacts on the parameter values compared for different lines of sight. The grain size distribution for this study was calculated by a code which uses the equations given by Li & Draine (2001, equations from 20 to 23). These equations have six adjustable parameters for carbonaceous grains and five for silicate grains. These parameters are the transition sizes ( $a_{t,g}, a_{t,s}$ ), upper cut-off parameters ( $a_{c,g}, a_{c,s}$ ), curvature parameters ( $\beta_g, \beta_s$ ), power law coefficients ( $C_g, C_s$ ) and powers ( $\alpha_g, \alpha_s$ ) for carbonaceous and silicate grains. The carbon abundance relative to hydrogen in very small grains (PAH) is given by  $b_c$ . For all models we have taken  $a_{c,s} = 0.1 \mu$ . The wavelength dependent extinction  $A(\lambda)$  per unit column density  $N(H)$  for the dust model is then calculated as:

$$A(\lambda) = \int Q_{\text{ext}}(a, \lambda) a^2 (dn/da) da,$$

integrating over the size distribution, where  $Q_{\text{ext}}(a, \lambda)$  is the extinction efficiency calculated for spherical dust grains of size ‘ $a$ ’ using BHMIE code (Bohren & Huffman 1983) which was called as a subroutine for the main code. The grain size distribution with sizes ‘ $a$ ’ and ‘ $a + da$ ’ is given as  $dn/da$ . The optical properties of astronomical silicate, graphite and PAH were adapted from <http://www.astro.princeton.edu/~draine>. PAH is composed with 50% neutral and 50% ionised species. Graphite extinction is assumed to have contributed by factors of 1/3 and 2/3 from the dielectric tensor for the electric field perpendicular and parallel to the  $c$ -axis respectively, which is sufficiently accurate for the extinction curve modelling (Draine & Malhotra 1993). The size and the optical properties of carbonaceous grains vary smoothly from the very small PAH grains to the classical graphite grains. Several model extinction curves were calculated by varying 12 parameters and the best fit values of these parameters were found by the code by minimizing the sum of the squares of the deviation between the theoretical and observed extinction curves. The size distributions of silicate, graphite and PAH are given as the output by the code. The albedo ‘ $\Omega$ ’ and the asymmetric parameter ‘ $g$ ’ (average of the angle through which the radiation is scattered by dust) for the considered dust model were computed by the code as the following:

$$\Omega = S/(S + A), \quad g = G/S,$$

where

$$S/N(H) = \int (dn/da) Q_{\text{sca}}(a, \lambda) a^2 da,$$

$$A/N(H) = \int (dn/da) Q_{\text{abs}}(a, \lambda) a^2 da,$$

$$G/N(H) = \int (dn/da) g Q_{\text{sca}}(a, \lambda) a^2 da,$$

with  $Q_{\text{sca}}(a, \lambda)$ ,  $Q_{\text{abs}}(a, \lambda)$  as the scattering and absorption coefficients respectively. The elemental abundances of carbon and silicon relative to hydrogen locked in the interstellar dust were also computed by the code by numerically integrating the following relation over the size distribution:

$$E = (4/3M)\pi\rho \int (dn/da)a^3 da, \quad (1)$$

where  $M$  is the mass number and  $\rho$  is the mass density of the element. The mass density of graphite is  $2.24 \text{ g cm}^{-3}$  and for silicate it is taken as  $3.5 \text{ g cm}^{-3}$ , an average value between the densities of crystalline forsterite and fayalite. The mass number per structural unit of silicate grain is 172. Abundances of magnesium, and iron are taken to be the same as the abundance of silicon. The abundance of oxygen is taken as four times of silicon abundance. While fitting the curves we took 900 points equally spaced in wavenumber  $\lambda^{-1}$  from 1 to 10.

## 4. Results and discussion

### 4.1 Average dust characteristics in the diffuse ISM ( $R_V = 3.1$ )

To determine the average dust characteristics in the diffuse ISM (DISM), we have modelled the mean ISM extinction curve obtained from the parameter values given by FM07. The mean extinction curve derived from the ‘extinction without standard’ method differs significantly from the extinction curve derived from the ‘pair method’ using Fitzpatrick (1999) parameterization (see Fig. 1). The main difference occurs in the UV and in the Far-UV regions of the extinction curve. The ‘pair method’ underestimates the continuum extinction at these wavelength regions. The strength and the width of the 2175 Å bump do not show any notable differences and the Far-UV rise is steeper in the curve derived from the ‘extinction without standard method’.

Figure 2(a) shows the best fit theoretical curve derived from our three-component dust model to the mean ISM extinction curve. The corresponding model parameters are given in Table 1. Figure 2(a) also shows the individual contribution from silicate, graphite and PAH components for the total extinction. The proposed model indicates that the silicate and graphite grains provide a major part of optical extinction as observed by WD01. However, our model predicts nearly equal contribution from both the components whereas WD01 model shows a larger contribution from silicate than from graphite. Silicate has steep, featureless continuum extinction down to  $\lambda = 0.15 \mu$  below which the extinction does not show a strong variation with wavelength. While silicate dominates the continuum extinction in the UV and in the Far-UV regions, the Far-UV rise in the extinction curve is caused mostly by PAH, with a little contribution from small silicate grains. Graphite displays a weak wavelength dependent continuum extinction from Optical to Far-UV regions. As it can be seen from Fig. 2(a), a major part of the 2175 Å absorption feature comes from the PAH grain composition with some contribution from graphite. The size distributions of the three dust components are shown in Fig. 2(b). Silicate grain size distribution rises from  $0.01 \mu$ , peaks at a size of  $0.198 \mu$  and then falls rapidly. PAH has the smallest size of  $3.5 \text{ \AA}$  and the two log normal size distributions are centered at sizes  $6 \text{ \AA}$  and  $50 \text{ \AA}$ . Classical graphite size distribution has a peak at  $0.264 \mu$ . PAH dominates the very small grain population and graphite dominates the carbonaceous dust in the ISM.

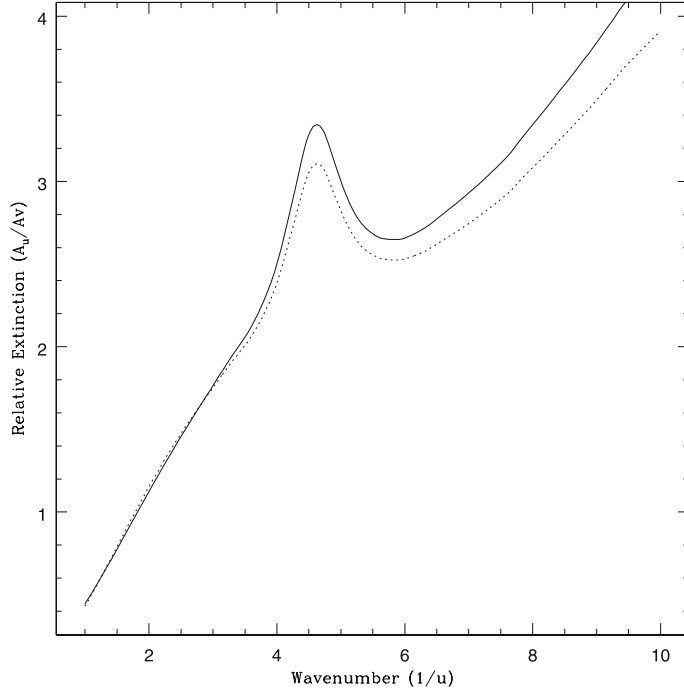


**Figure 1.** Mean ISM extinction curves derived from standard ‘pair method’ (dotted line) and from ‘extinction without standard method’ (solid line) showing significant differences in the UV and Far-UV regions.

The abundances of silicon, carbon and oxygen locked in the diffuse ISM dust are derived from our model and the values are given in Table 2. The derived abundances are consistent with the available abundances of these elements in the ISM dust and it shows a closer agreement with the F & G type stars surface composition for the ISM than with the solar abundance. Similar conclusion was reached by Zubko *et al.* (2004) by simultaneously fitting the extinction curve and diffuse IR emission. The carbon abundance in our dust model is significantly lower than the required carbon for the MRN model which needs almost all the carbon available in the ISM. Our model predicts the same amount of carbon in PAH (60 ppm) reported by WD01. Silicon abundance derived in this work is significantly lower than the value given by WD01. The variation of albedo and the asymmetry parameter with wavelength in our ISM dust model are given in Fig. 2(c) and Fig. 2(d) respectively. The albedo peaks at 5880 Å and both the curves show dip at 2175 Å. Shorter wavelength calculation of the extinction curve shows another bump at 950 Å which is stronger than the 2175 Å feature and is also contributed mostly from PAH (see Fig. 3). The signatures of this absorption feature are also seen in the albedo and asymmetry parameter curves at the same wavelength.

#### 4.2 Dust along the line of sight to HD 210121 ( $R_V = 2.1$ )

To examine and compare the dust characteristics at distinct environmental regions in the Galaxy, we have taken the extinction curve for which the line of sight passes through

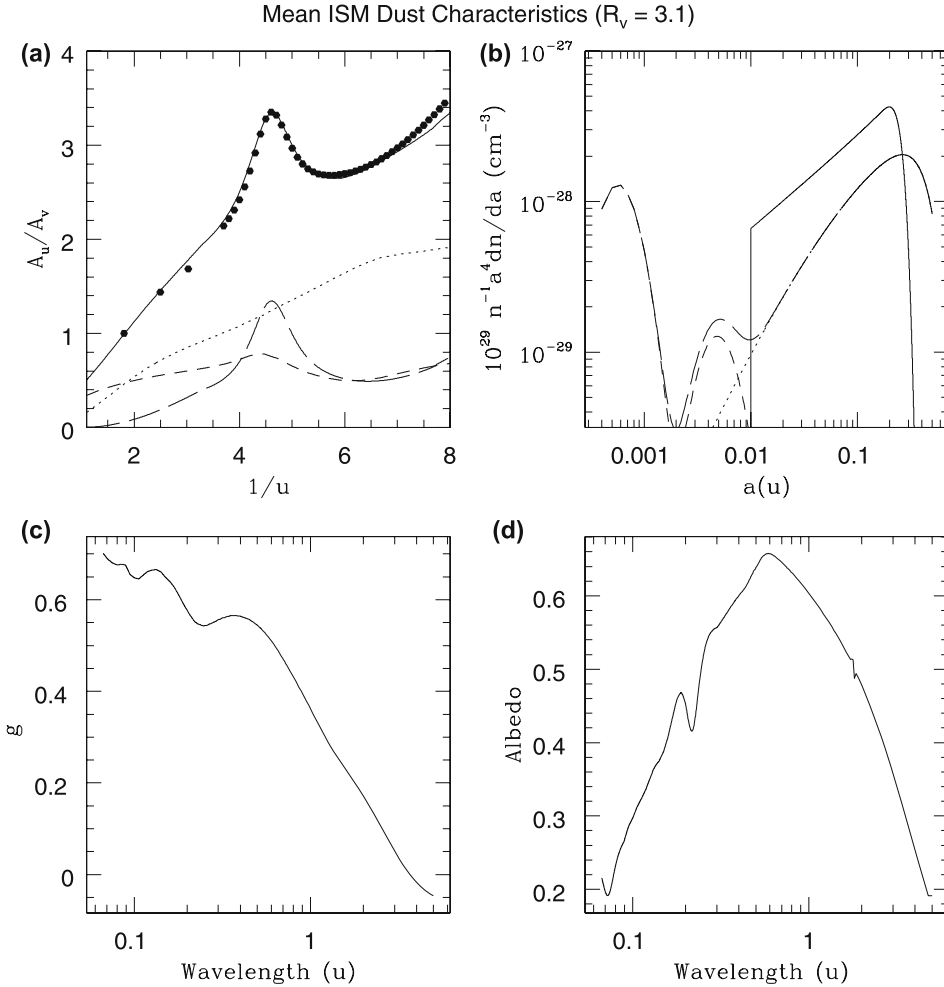


**Figure 2.** (a) Mean ISM extinction curve (points) fitted with a three-component dust model (solid line). Contributions from silicate (dotted line), graphite (short dashed line) and from PAH (long dashed line) are shown; (b) grain size distribution for silicate (solid line), graphite (dotted dashed line) and PAH (short dashed line) are shown; (c) variation of scattering parameter 'g' with wavelength; and (d) variation of albedo with wavelength for the given dust model.

a high Galactic latitude diffuse molecular cloud towards HD 210121. These clouds are translucent clouds representing the transition regions between diffuse clouds, in which the chemistry is driven primarily by photoprocesses and dark clouds, in which the collisional processes dominate the reaction network. This line of sight has a very small value of  $R_V$  and is one among the cases which deviate substantially from the parameterisation of Galactic extinction curves by CCM showing a weaker 2175 Å bump and a stronger Far-UV rise than expected. Extinction along this sight line was studied earlier by several authors (Welty & Fowler 1992; Larson *et al.* 2000 and WD01) and all these studies were made with the observed extinction derived from the standard 'pair method'.

**Table 1.** Model parameters for best fit three-component dust models to the observed extinction at different interstellar environments.

Region	$\alpha_g$	$\beta_g$	$a_{t,g}(\mu)$	$a_{c,g}(\mu)$	$C_g$
DISM	-1.55	-0.165	0.0107	0.428	$9.99 \times 10^{-12}$
HD 210121	-1.69	-0.264	0.0126	0.449	$8.6 \times 10^{-12}$
HD 37022	-1.62	-0.721	0.0418	0.720	$7.58 \times 10^{-13}$
Region	$\alpha_s$	$\beta_s$	$a_{t,s}$	$C_s(\mu)$	
DISM	-2.4	0.10	0.164	$8.0 \times 10^{-13}$	
HD 210121	-2.26	-20	0.119	$2.3 \times 10^{-12}$	
HD 37022	-1.63	2.15	0.193	$3.2 \times 10^{-14}$	

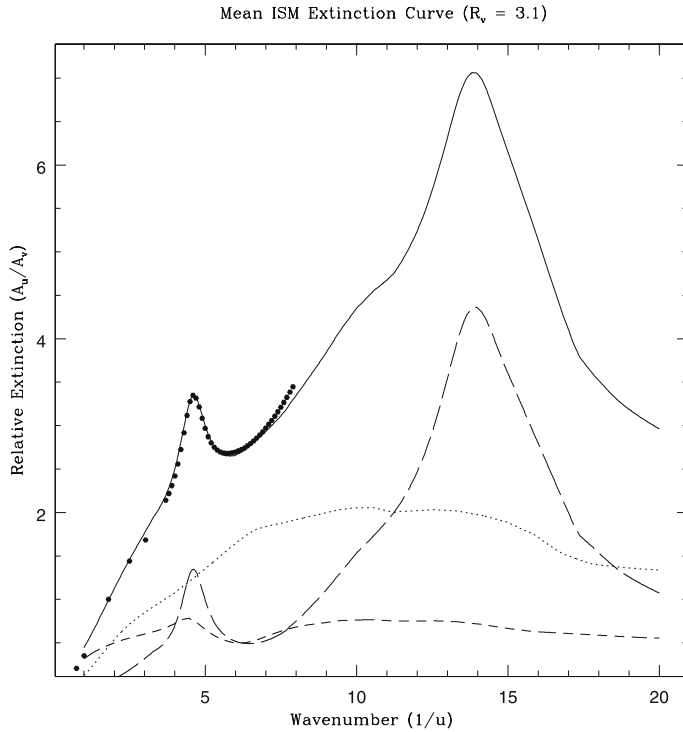
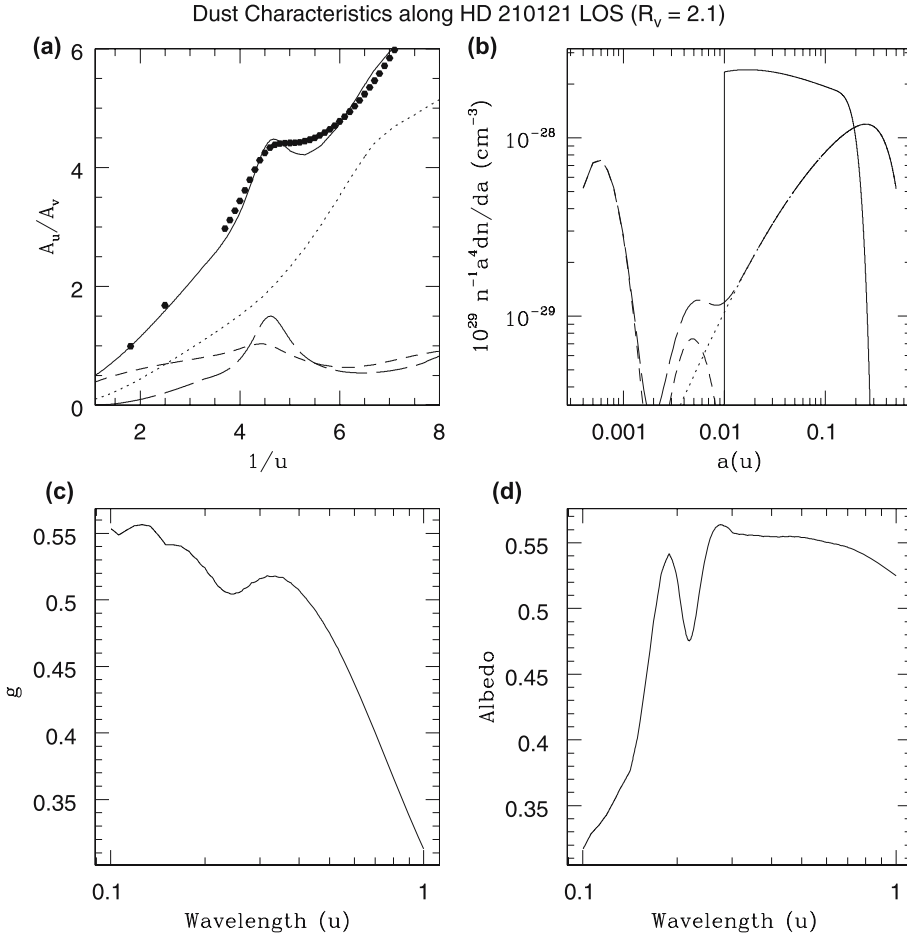
**Figure 3.** Mean ISM extinction curve (points) fitted with a three-component dust model (solid line). Contributions from silicate (dotted line), graphite (short dashed line) and from PAH (long dashed line) computed down to the Lyman limit are shown.

Figure 4(a) shows the observed extinction obtained from the ‘extinction without standard method’ and the best fit theoretical curve derived from silicate/graphite/PAH dust model to the observation. Contributions from individual dust components for the total extinction are also shown in the figure. In Table 1 we list the model parameters of our best fit model to the extinction curve. Our results show that the extinction



**Figure 4.** (a) Extinction curve along the line of sight of high latitude cloud HD 210121 (points) fitted with a three-component dust model (solid line). Contributions from silicate (dotted line), graphite (short dashed line) and from PAH (long dashed line) are shown; (b) grain size distribution for silicate (solid line), graphite (dotted line) and PAH (short dashed line) are shown; (c) variation scattering parameter ‘ $g$ ’ with wavelength; and (d) variation of albedo with wavelength for the given dust model.

in UV and in Far-UV regions are dominated by silicate grains, silicate and graphite grains contribute comparatively for the Optical extinction. Silicate has featureless steep continuum extinction and even in the Far-UV region the extinction is strongly dependent on the wavelength, unlike in the case of the mean ISM. Graphite shows a weak wavelength dependent extinction from Optical to the Far-UV. The 2175 Å bump is mostly coming from PAH with some contribution from graphite. The Far-UV extinction is almost given by silicate and it is much larger than the derived value for the average ISM. This is expected if there is an excess amount of very small grains as suggested by previous studies (Larson *et al.* 2000). The excess of very small grains towards this line of sight can also be seen from the size distribution (see Fig. 4b). Silicate grain size increases from  $0.01 \mu$ , the size distribution soon attains a peak at  $0.017 \mu$  and falls off rapidly after  $0.14 \mu$ . This shows a larger amount of small silicate

**Table 2.** Elemental abundances in dust at different environmental regions of the Galaxy. References to the abundances are H01: Holweger (2001); SM01: Sofia & Meyer (2001); C96: Cardelli *et al.* (1996).

Region	Carbon (ppm)	Oxygen (ppm)	Silicon (ppm)	$b_c$ (ppm)
Solar (H01)	$391 \pm 98$	$545 \pm 100$	$34.4 \pm 3.9$	–
F & G stars (SM01)	$358 \pm 82$	$445 \pm 156$	$39.9 \pm 13.1$	–
DISM Gas (C96)	$108 \pm 16$	$319 \pm 14$	$\sim 0$	–
Dust in DISM (MRN)	370	–	35	–
Dust in DISM (WD01)	252	–	48	60
Dust in DISM (this work)	253	148	37	60
Dust along HD 210121 LOS (WD01)	165.8	–	52.3	40
Dust along HD 210121 LOS (this work)	162	140	35	35
Dust along HD 37022 LOS (this work)	156	172	43	18

grains and a smaller amount of classical silicate grains existing along this sightline in contrast to the diffuse ISM. The size distribution of graphite peaks at  $0.25 \mu$ , similar to the mean ISM. PAH has a minimum size of  $3.5 \text{ \AA}$  and follows two log normal size distributions with their peaks located at  $6 \text{ \AA}$  and  $50 \text{ \AA}$ . Carbonaceous grains hence display a similar size distribution towards HD 210121 and in the diffuse ISM.

The abundances of carbon, oxygen and silicon locked in the dust grain along the sightline of HD 210121 were derived from our model and the values are given in Table 2. Silicon abundance is comparable with (95% of) the average value in ISM dust, however the total carbon abundance is significantly lower, only 65% of the ISM value. This is in contrast with the dust abundances derived from the two component dust model by Larson *et al.* (2000) which uses all Solar abundance of silicate. Larson *et al.* (2000) dust model needed a carbon abundance of 216 ppm. Carbon abundance in PAH in our model (see Table 2) is considerably lower than the value obtained for the diffuse ISM. While the steeper Far-UV rise was fitted by the excess of small silicate grains, the weaker  $2175 \text{ \AA}$  feature is fitted by the smaller amount of PAH along this sightline. Hence the main difference in dust properties along this sightline from the mean ISM dust comes from the carbon abundance in carbonaceous grains and the silicate size distribution. The variation of asymmetry parameter and albedo with wavelength for the proposed dust model are given in Fig. 4(c) and in Fig. 4(d) respectively. Both the plots show dip at  $2175 \text{ \AA}$ . The albedo peaks at much shorter wavelength ( $2755 \text{ \AA}$ ) than seen for the diffuse ISM. Signatures of the absorption feature at  $950 \text{ \AA}$  are seen both in asymmetry parameter and in albedo.

#### 4.3 Dust along the line of sight to HD 37022 ( $R_V = 6.42$ )

To investigate the dust characteristics in a dense interstellar environment using our three-component dust model, we have chosen extinction along the line of sight of HD 37022 which is a member in the cluster NGC 1977. This sightline has an unusually

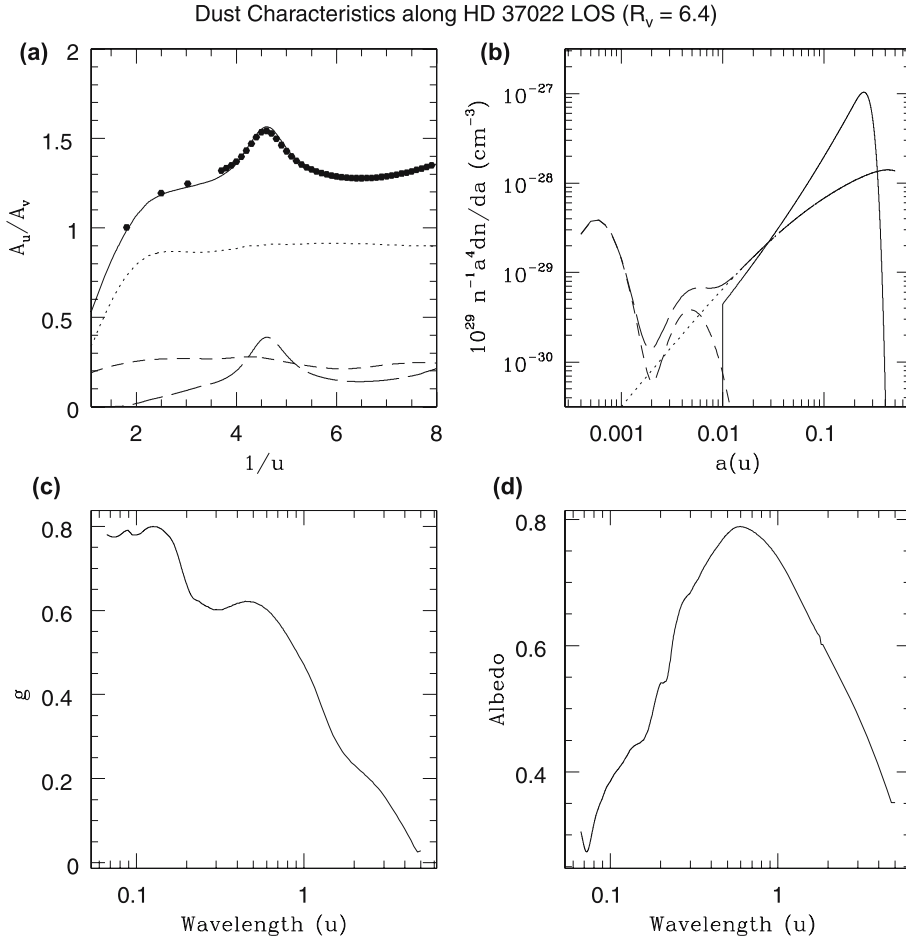


**Figure 5.** (a) Extinction curve along the line of sight of HD 37022 (points) fitted with a three-component dust model (solid line). Contributions from silicate (dotted line), graphite (short dashed line) and from PAH (long dashed line) are shown; (b) grain size distribution for silicate (solid line), graphite (dotted dashed line) and PAH (short dashed line) are shown; (c) variation of scattering parameter ‘ $g$ ’ with wavelength; and (d) variation of albedo with wavelength for the given dust model.

large value of  $R_V$ . In Fig. 5(a) the observed extinction derived from the ‘extinction without standard’ method is shown. The curve displays significant differences from the mean ISM extinction by showing a weak 2175 Å bump and a grey continuum extinction in the UV and Far-UV regions. Figure 5(a) also displays the theoretical extinction computed from a three-component dust model for the observed curve. Contributions from silicate, graphite and PAH components for the total extinction are also shown in the figure. In Table 1 we list the model parameters of our best fit dust model to the extinction curve. As it can be seen silicate grains dominate the extinction from Optical, UV as well as the Far-UV regions. Silicate extinction rises steeply in the optical domain (steeper than for mean ISM and HD 210121 sight lines) down to a wavelength  $0.5 \mu$  below which it shows a wavelength independent extinction unlike for the case of mean ISM and HD 210121 sightline. Graphite shows a wavelength independent extinction

throughout the wavelength region from Optical to Far-UV. The 2175 Å bump is mostly given by PAH composition. Silicate size distribution rises steeply from  $a = 0.01 \mu$ , attains a maximum at size  $a = 0.246 \mu$  and then falls rapidly (see Fig. 5b). Graphite size distribution peaks at size  $a = 0.425 \mu$ . The peak sizes of silicate and graphite are larger than their respective values for the diffuse ISM indicating a growth of classical grains at this dense environment. PAH grains have a minimum size of 3.5 Å and follow two log normal size distributions with their peaks located at 6 Å and 50 Å.

The derived abundances of carbon, oxygen and silicon locked in dust along the line of sight of HD 37022 are listed in Table 2. Carbon abundance is significantly lower than (62% of) the diffuse ISM value and only 18 ppm among the total carbon abundance is in the form of PAH. Silicate abundance along this line of sight is 16% larger than the derived value for the diffuse ISM. The asymmetry parameter and the albedo for the proposed dust model are plotted against wavelength in Fig. 5(c) and Fig. 5(d) respectively. The albedo peaks at 5950 Å, not significantly larger than the mean ISM value. Unlike the case of the ISM the albedo does not show a noticeable dip at 2175 Å while it is seen in asymmetry parameter. Signatures of the absorption feature at 950 Å are seen both in asymmetry parameter and in albedo.

## 5. Conclusions

From this study, it is concluded that the three-component dust model comprising silicate, graphite and PAH applied to the extinction curves derived without using standard stars can give consistent explanation for the variation of Galactic extinction curves providing the dust properties along the line of sight including the elemental abundances in dust. Mean ISM dust abundances are better matched to the expectation of solid state material in the ISM if the atmospheric abundances of F & G type stars are assumed for the ISM rather than the solar. Characteristics of the interstellar dust at different environments are examined and compared by applying this dust model to the extinction curves along three different lines of sight, namely, (a) to the mean ISM, (b) to a line of sight passing through a high latitude diffuse molecular cloud towards HD 210121 with a lowest value of  $R_V$ , and (c) to a line of sight passing through a dense interstellar environment towards HD 37022 with a large value of  $R_V$ .

Measurements of carbon and silicon abundances in the interstellar gas have set a value of  $\sim 110$  ppm (Cardelli *et al.* 1996; Mathis 2000) and 17 ppm (Snow & Witt 1996) respectively. The atmospheric abundances of carbon and silicon in B type stars are estimated to be 190 ppm and 18.8 ppm respectively (Sofia & Mayer 2001). Mathis (1996) has reviewed the constraints on the interstellar dust models based on the expected abundances of the ISM and indicated that the strengths of 9.7  $\mu$  and 18  $\mu$  silicate features require atleast the solar abundance of silicon. Infrared emission features require a carbon abundance of 60 ppm in PAH. These observations provide serious difficulty for the interstellar abundance budget if the atmospheric abundances of B type stars are taken for the ISM. Mathis (1996) has discussed that 69% of solar abundances for the heavy element content of the ISM may be compatible with the observations setting a value of  $C/H = 170$  ppm (taking 38% of carbon is in gas, Mathis 1996). Classical grains with vacuum included can provide the needed extinction with less amount of solid materials (Vaidya *et al.* 2007). Consideration of such porous spheroidal grains in addition to the methodology described in this work is in progress. However, for a

study comparing the dust properties at different interstellar environments made here and by WD01, the filled spherical grains assumption is adequate.

### Acknowledgements

The author acknowledges Mr. Y. Bharat Kumar and Ms. G. Priya for their help.

### References

- Allamandola, L. J., Tielens, A. G. G. M., Barker, J. R. 1985, *ApJ*, **290**, L25.  
 Bless, R. C., Seavage, B. D. 1972, *ApJ*, **171**, 293.  
 Bohren, C. F., Huffman, D. R. 1983, Absorption and scattering of light by small particles (New York: Wiley).  
 Cardelli, J. A., Clayton, G. C., Mathis, J. S. 1989, *ApJ*, **345**, 245 (CCM).  
 Cardelli, J. A., Meyer, D. N., Jura, M., Seavage, B. D. 1996, *ApJ*, **467**, 334.  
 Draine, B. T., Anderson, N. 1985, *ApJ*, **292**, 494.  
 Draine, B. T., Malhotra, S. 1993, *ApJ*, **414**, 632.  
 Draine, B. T., Lazarian, A. 1998, *ApJ*, **508**, 157.  
 Fitzpatrick, E. L., 1999, *PASP*, **111**, 63.  
 Fitzpatrick, E. L., Massa, D. 1986, *ApJ*, **307**, 286.  
 Fitzpatrick, E. L., Massa, D. 1988, *ApJ*, **328**, 734.  
 Fitzpatrick, E. L., Massa, D. 2005, *ApJ*, **130**, 1127.  
 Fitzpatrick, E. L., Massa, D. 2007, *ApJ*, **663**, 320.  
 Holweger, H. 2001, In: Joint SOHO/ACE workshop ‘Solar and Galactic Composition’, (ed.) Wimmer-Schweingruber R.F., American Institute of Physics Conf. Proceedings, **598**, 23.  
 Larson, K. A., Wolff, M. J., Roberge, W. G., Whittet, D. C. B., He, L. 2000, *ApJ*, **532**, 1021.  
 Li, A., Draine, B. T. 2001, *ApJ*, **554**, 778.  
 Li, A., Greenberg, J. M. 1997, *A&A*, **232**, 566.  
 Mathis, J. S. 1996, *ApJ*, **472**, 643.  
 Mathis, J. S. 2000, *JGR*, **105**, 10269.  
 Mathis, J. S., Rumpl, W., Nordsieck, K. H. 1977, *ApJ*, **217**, 425 (MRN).  
 Snow, T. P., Witt, A. N. 1996, *ApJ*, **468**, L65.  
 Sofia, U. J., Meyer, D. M. 2001, *ApJ*, **554**, L221.  
 Stecher, T. P. 1965, *ApJ*, **142**, 1683.  
 Vaidya, D. B., Gupta, R., Snow, T. P. 2007, *MNRAS*, **379**, 791.  
 Weingartner, J. C., Draine, B. 2001, *ApJ*, **548**, 296 (WD01).  
 Welty, D. E., Fowler, J. R. 1992, *ApJ*, **393**, 193.  
 Zubko, V., Dwek, E., Arendt, R. G. 2004, *ApJS*, **152**, 211.